JOURNAL OF AGRICULTURAL AND FOOD CHEMISTRY

Monitoring the Binding Processes of Black Tea Thearubigin to the Bovine Serum Albumin Surface Using Quartz Crystal Microbalance with Dissipation Monitoring

MONTHANA CHITPAN, XIAOYONG WANG, CHI-TANG HO, AND QINGRONG HUANG*

Department of Food Science, Rutgers University, 65 Dudley Road, New Brunswick, New Jersey 08901-8520

The binding processes of thearubigin, which is one of the two major polyphenols (the other one is theaflavin) that gives black tea its characteristic color and taste, to the bovine serum albumin (BSA) surface have been investigated by quartz crystal microbalance with dissipation monitoring (QCM-D). The mass and thickness of the thearubigin adlayer on BSA surfaces at various thearubigin concentrations, salt concentrations, and pH values have been determined by QCM-D using the Voigt model. Our results show that the adsorption isotherm of thearubigin on the BSA surface can be better described by the Langmuir model than the Freundlich model, suggesting that the thearubigin adsorption on the BSA surface is dominated by specific interactions, such as electrostatic interaction and hydrogen bonding, as evidenced by the stronger thearubigin adsorption at pH below the isoelectric point (p*I*) of BSA and shifts in the positions of both amide bands in the FTIR spectra of the BSA surface with and without thearubigin adsorption. The addition of salt can also influence the thearubigin binding to BSA surfaces. The salt concentration-enhanced effect at a salt concentration lower than 0.1 M is explained as that an increase of salt concentration can screen the electrostatic repulsion to a larger extent than the electrostatic attraction between thearubigin and BSA. On the other hand, when the salt concentration is higher than 0.1 M, both electrostatic repulsion and attraction can be significantly screened by the higher salt concentration, resulting in the salt concentration-reduced effect. However, when the salt concentration is further increased to 0.4 M, the addition of thearubigin may promote the formation of a certain type of complex with BSA, resulting in the increases of both thickness and mass of the thearubigin adlayer.

KEYWORDS: Thearubigin; salt-enhanced and salt-reduced effects; electrostatic interaction; quartz crystal microbalance with dissipation monitoring (QCM-D)

INTRODUCTION

Tea refers to the plant *Camellia sinesis*, its leaves, and the extracts and infusion thereof. Tea, consumed by over two-thirds of the world's population, is now the second most popular beverage, next only to water (*1*). Black teas and green teas are the two main types, defined by their respective manufacturing techniques. Polyphenols, in particular the catechins, are the most significant group of tea components (*2, 3*). During the production of black tea, the fermentation (enzymatic oxidation) processes cause green tea catechins to oxidize and polymerize to form oligomeric flavanols, including theaflavins, thearubigin, and other oligomers (*4*). Theaflavins and thearubigin are two main polyphenols that give black tea its characteristic color and taste (*5*). The structure of thearubigin, the most abundant phenolic fraction in black tea with molecular weight ranging from 1000 to 40000, has not yet been well characterized (*6*). Recent studies show that black tea polyphenols have numerous health benefits, including the prevention of chronic diseases such as cancer and cardiovascular diseases (*7–12*).

Tea polyphenols have been reported to interact with proteins. Epigallocatechin-3-gallate (EGCG), the most abundant catechin in green tea, was found to bind to salivary proline-rich protein, which may be responsible for the astringency tastes of tea (*13, 14*). The interactions between EGCG and proline-rich protein take place because the A and D (gallate group) rings of EGCG interact with proline (*15*). The interactions can be either reversible or irreversible, depending on pH, temperature, and the concentration of either protein or flavonoid (*2*). Some studies reported that the interactions between polyphenols in tea and proteins might lead to the loss of bioavailability of polyphenols and their antioxidant capacity (*16*). Previous results showed the reduced risk of coronary heart disease in subjects drinking black tea alone, but no beneficial effects were observed in subjects

* Author to whom correspondence should be addressed (telephone, 732-932-7193; fax, 732-932-6776; e-mail, qhuang@aesop.rutgers.edu).

10.1021/jf072236t CCC: $37.00
Published on Web 11/22/2007

consuming black tea with milk (*16*). Arts et al. reported that casein had negative effects on the antioxidant capacity of green tea and black tea polyphenols (*2a*).

The aim of this paper is to understand the mechanism involved in the intermolecular interactions between black tea thearubigin and bovine serum albumin (BSA), which is a globular protein which functions biologically as a carrier for fatty acid anions and other simple amphiphiles in the bloodstream (*17*). One BSA molecule contains 583 amino acids in a single polypeptide chain with a molecular weight of about 66000 (*18*). Quartz crystal microbalance (QCM) is an extremely sensitive mass sensor capable of measuring the mass changes of a material at the level of 0.4 ng/cm^2. The detection signals and calculated adsorbed mass in the conventional QCM are solely based on the assumption that the changes of the fundamental frequency of piezoelectric is proportional to the change of adsorbed mass on the surface of the quartz crystal calculated from the classical Sauerbrey equation (*19*). However, it is now known that the changes of the fundamental frequencies of quartz crystals depend not only on the mass adsorbed on the quartz crystal surfaces but also on other factors, such as temperature and viscoelastic properties of the adlayers (*20*). In many systems involving biomolecules, the adsorbed film is not rigid, making the Sauerbrey relation invalid. A film that is "soft" (viscoelastic) will not fully couple to the oscillation of the crystal, which dampens the crystals oscillation. The conventional QCM has limits for precise mass detection in the liquid environment because the mass obtained is very often underestimated (*21, 22*). The improved QCM with dissipation monitoring, also called QCM-D, has been shown to provide a better tool to investigate viscoelastic soft materials since it also takes into account the energy dissipation factor (*23*). Previously, conventional QCM was used to monitor the binding kinetics between bovine serum albumin and tannic acid (*24*). Very recently, we employed QCM-D to study the interactions between (−)-epigallocatechin gallate (EGCG) and the bovine serum albumin (BSA) surface (*25*). Our results showed that the EGCG adsorption on the BSA surface was dominated by nonspecific hydrophobic interaction.

As an extension of our previous work on EGCG, we will further explore the effect of polyphenol structure (i.e., the charge-containing polyphenol like thearubigin) on polyphenol binding to the BSA surface. In this paper, QCM-D is used to monitor the binding of black tea thearubigin to the BSA surface in real time, where BSA is chemically immobilized on the gold-coated quartz crystal surface. The adsorbed mass, thickness of the thearubigin adlayer on the BSA surface at various thearubigin concentrations, pH values, temperatures, and salt concentrations are determined by a combination of QCM-D and the Voigt model. A novel mechanism regarding the effects of salt concentration on the binding of thearubigin to BSA is proposed.

MATERIALS AND METHODS

Materials. Bovine serum albumin (BSA, ≥98% pure by gel electrophoresis) was purchased from Sigma Chemical Co. (St. Louis, MO) and used without further purification. 11-Mercaptoundecanoic acid (11-MUA) (Aldrich, St. Louis, MO), *N*-hydroxysuccinimide (NHS) (Aldrich), 1-ethyl-3-(3-dimethylaminopropyl)carbodiimide hydrochloride (EDC) (Sigma), acetic acid (Aldrich), sodium acetate (Fisher, Fair Lawn, NJ), ammonium hydroxide (NH_4OH) (VWR, West Chester, PA), hydrogen peroxide (H_2O_2) (Aldrich), sodium chloride (NaCl) (Fisher), and absolute ethanol (Fisher) were all used as received. The buffers used were acetate buffers of 0.001, 0.01, 0.1, 0.15, 0.2, and 0.4 M at pH 4.9 and 0.01 M at pH 3, as well as sodium phosphate buffer of 0.01 M at pH 7.

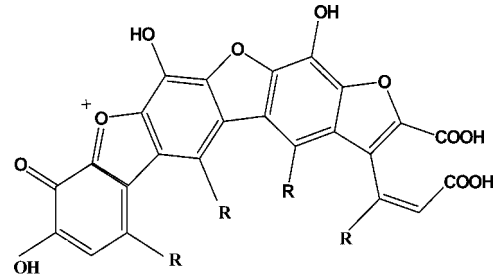

Figure 1. Possible dimeric structure of thearubigin proposed by Haslam (*5*) to account for its color and acidity.

Preparation of Thearubigin. Five grams of black tea water-soluble powder (a gift from Unilever Co., Englewood Cliffs, NJ) was dissolved in 200 mL of water. It was extracted with 200 mL of ethyl acetate for three times. The water layer was then extracted with 200 mL of butanol for three times. The combined butanol extract was dried using a rotary evaporator under vacuum. Thearubigin (1.2 g) was obtained. The possible dimeric structure of thearubigin proposed by Haslam (*5*) to account for its color and acidity is shown in **Figure 1**. The extracted thearubigin was then dissolved in 0.01 M acetate buffer at pH 4.9 to prepare thearubigin solutions with concentrations of 0.002%, 0.005%, 0.02%, 0.032%, 0.08%, 0.15%, and 0.30%, respectively.

Preparation of the BSA Surface. AT-cut gold-coated quartz crystals (fundamental frequency of 5 MHz) were purchased from Q-Sense AB (Sweden). The immobilization of BSA on the gold-coated quartz crystal surface was carried out using the procedure modified from a previously published paper (*26*). Gold-coated quartz crystals were first cleaned in an UV/ozone chamber for 10 min, followed by immersion in a 1:1:5 mixture of ammonium hydroxide (NH_4OH, 25%), hydrogen peroxide (H_2O_2, 30%), and Milli-Q water for 5 min at 75 °C, and finally cleaned in an UV/ozone chamber for another 10 min These gold-coated quartz crystals were then rinsed with a large quantity of Milli-Q water, dried with nitrogen gas (N_2), and subsequently soaked in 10 mM 11-mercaptoundecanoic acid (11-MUA)/absolute ethanol solution at 60 °C for at least 24 h. The excess amount of 11-MUA was rinsed off with absolute ethanol, and the modified quartz crystal surfaces were dried under N_2 flow. Just before the immobilization of protein, 11-MUA-coated quartz crystal surfaces were activated by a mixed solution containing 1:1 (v/v) of 100 mg/mL 1-ethyl-3-(3-dimethylaminopropyl) carbodiimide hydrochloride (EDC) and 100 mg/mL *N*-hydroxysuccinimide (NHS) in Milli-Q water for 1 h. The solution of 10 mg/mL BSA in phosphate buffer (pH 7.0) was used to incubate the activated surfaces at 4 °C for at least 24 h. The quartz crystal surfaces were finally rinsed thoroughly by phosphate buffer, followed by Milli-Q water, and dried under N_2 flow.

FTIR Measurements. The infrared spectra of BSA-modified quartz crystal surfaces before and after thearubigin adsorption were collected with a Thermo Nicolet smart apertured grazing angle (SAGA) accessory operating at the grazing angle of incidence of 80°. Both ATR and grazing angle measurements were carried out using a Fourier transform infrared spectrometer (Thermo Nicolet 670, Madison, WI). The resolution was set to 4 cm^{-1}, and 1024 scans were collected for each sample.

QCM-D Measurements. The interactions between thearubigin and the BSA functionalized quartz crystal surface were studied using a commercial QCM-D apparatus (Q-Sense AB, Sweden) with a Q-Sense D300 electronic unit. A polypropylene pipet tip connecting to the temperature-controlled chamber was initially filled with the specific buffers studied. By opening the valve, distilled water was exchanged in the QCM-D chamber via the gravitational flow. After a stable baseline was established, polyphenol solutions in water were exposed to the BSA-modified crystal surface. At the same time, the adsorption was monitored as a function of time by recording the shifts in both frequency (ΔF) and energy dissipation (ΔD) simultaneously at the fundamental resonant frequency along with the third, fifth, and seventh overtones

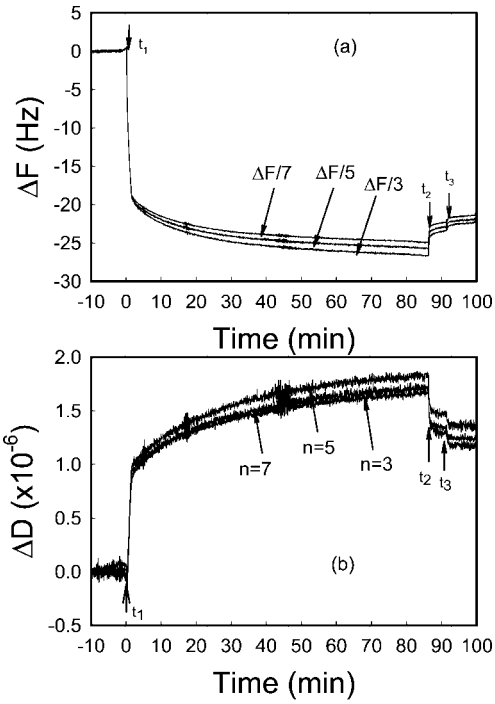

Figure 2. (a) Frequency shift (ΔF) and (b) energy dissipation shift (ΔD) induced by the adsorption of 0.032% thearubigin acetate buffer solution at pH = 3.0 and I = 0.01 M on the bovine serum albumin-coated quartz crystal surface. ΔF and ΔD are measured simultaneously at three overtones (n = 3, 5, 7) and normalized by their overtone number. The arrows indicate the time for the injection of thearubigin molecules (t_1) and two times of rinsing steps (t_2 and t_3).

until the steady state of the adsorption was reached. The long-term stability of the frequency was within 1 Hz, and this drift was negligible compared to the frequency shifts due to the adsorption.

Traditionally, Sauerbrey mass was calculated from the Sauerbrey equation (*19*):

$$M = -\frac{C}{n}\Delta F \tag{1}$$

ΔF, M, and n represent the frequency change, adsorbed mass per unit area, and overtone number, respectively. C is the mass sensitivity constant (17.7 ng/cm^2 Hz). The Q-Sense software determines the resonance frequency and the decay time τ_0 of the exponentially damped sinusoidal voltage signal over the crystal, and the dissipation factor D can be obtained from the equation:

$$D = \frac{1}{\pi f_0 \tau_0} = \frac{2}{\omega \tau_0} \tag{2}$$

where f_0 is the resonance frequency and τ_0 is the decay time.

RESULTS AND DISCUSSION

Effect of Thearubigin Concentration. The typical adsorption process of thearubigin on the bovine serum albumin (BSA) surface was monitored in real time by simultaneously measuring resonance frequency shifts (ΔF) and energy dissipation shifts (ΔD). Panels **a** and **b** of **Figure 2** show ΔF and ΔD changes as a function of time upon the addition of 0.032% thearubigin at pH 3.0 and in 0.01 M acetate buffer solution. The ΔF values obtained at three different overtones (n = 3, 5, 7) were normalized by their overtone number. The arrows indicate the injection time of the thearubigin solution (t_1) and several times of rinsing with buffer solutions (t_2, t_3), respectively. Right after the injection of the thearubigin solution, there is a rapid decrease in ΔF and a marked increase in ΔD, followed by a more gradual change in ΔF and ΔD until the steady state is reached. The adsorption of thearubigin on the BSA surface consists of reversible and irreversible adsorption processes. We use the data that were obtained after two times of rinsing to explain the reversible adsorption process. During the rinsing processes (t_2, t_3), the small amount of adsorbed thearubigin mass decreased, as indicated by the small increase in ΔF. At the same time, ΔD decreased slightly, suggesting that the thearubigin molecules were loosely adsorbed on the BSA surface, and the loss of the small amount of thearubigin molecules made the thearubigin adlayer more rigid. Although the reversible thearubigin adlayer can be washed out by the buffer rinsing processes, the irreversible adsorption may be the main driving force that causes the loss of antioxidant activities of thearubigin. The irreversible adsorption of thearubigin on the BSA surface is mainly caused by specific interactions, such as hydrogen bonding and electrostatic interaction, and will be discussed in detail in the following sections of this paper.

The Sauerbrey equation is in fact derived from uniform ultrathin rigid films with material properties indistinguishable from those of the quartz crystal. For an ideal rigid film, the ratios of the frequency shift with the overtone number ($\Delta F_n/n$) at different overtones should be overlapped with each other ($\Delta F_3/3 = \Delta F_5/5 = \Delta F_7/7$). However, a film that is "soft" (viscoelastic) will not fully couple to the oscillation of the quartz crystal, which dampens the crystal's oscillation. Therefore, the Sauerbrey equation will no longer be valid in the calculation of the adsorbed mass and thickness. Viscoelastic propertiy changes in the adsorbed materials on the electrode surface would create additional frequency shifts besides the ones due to the mass load on the electrode surface (*27*). The decreases in ΔF and the increases in ΔD indicate the mass increase of the adsorbed thearubigin adlayers and the formation of loose thearubigin adlayers on the BSA surface, respectively.

By taking into account the viscoelastic properties of the system, the Voigt model can allow a more accurate estimation of mass changes using QCM-D responses (*28*). In this model, ΔF and ΔD of an adsorbed layer can be concisely expressed using the equations:

$$\Delta F \approx -\frac{1}{2\pi\rho_0 h_0}\left[\frac{\eta_3}{\delta_3} + h_1\rho_1\omega - 2h_1\left(\frac{\eta_3}{\delta_3}\right)^2 \frac{\eta_1\omega^2}{\mu_1^{\,2} + \omega^2\eta_1^{\,2}}\right] \tag{3}$$

$$\Delta D \approx \frac{1}{\pi f \rho_0 h_0}\left[\frac{\eta_3}{\delta_3} + 2h_1\left(\frac{\eta_3}{\delta_3}\right)^2 \frac{\eta_1\omega^2}{\mu_1^{\,2} + \omega^2\eta_1^{\,2}}\right] \tag{4}$$

where ρ_0 and h_0 are the density and thickness of the crystal, respectively, η_3 is the viscosity of the bulk fluid, δ_3 [$=(2\eta_3/\rho_3\omega)^{1/2}$] is the viscous penetration depth of the shear wave in the bulk fluid, ρ_3 is the density of the bulk fluid, and ω is the angular frequency of the oscillation. Here, four unknown parameters of the adsorbed layer including the thickness, density, viscosity, and elastic shear modulus are represented by h_1, ρ_1, η_1, and μ_1, respectively. Because the adsorbed layer exhibits different penetration depth of harmonic acoustic frequencies, ΔF and ΔD are measured simultaneously at the fundamental resonant frequency along with the third, fifth, and seventh overtones. As a result, up to eight experimental values of ΔF and ΔD are available. The Q-Sense software, which is based on the Voigt model, has been used to model the responses at the third, fifth, and seventh overtones during the process of thearubigin

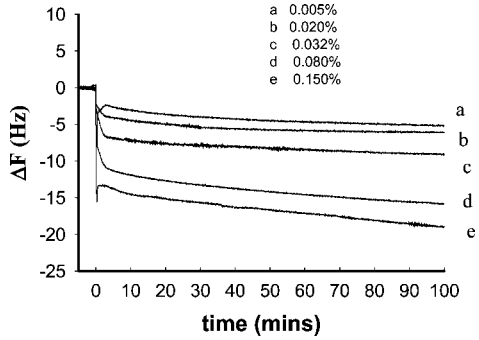

Figure 3. Time-dependent frequency shifts (ΔF) for thearubigin adsorption on BSA-modified quartz crystal surfaces for thearubigin solutions of various concentrations: (a) 0.005%; (b) 0.02%; (c) 0.032%; (d) 0.08%; (e) 0.15%. The thearubigin solutions were prepared in 0.01 M acetate buffer at pH = 4.9.

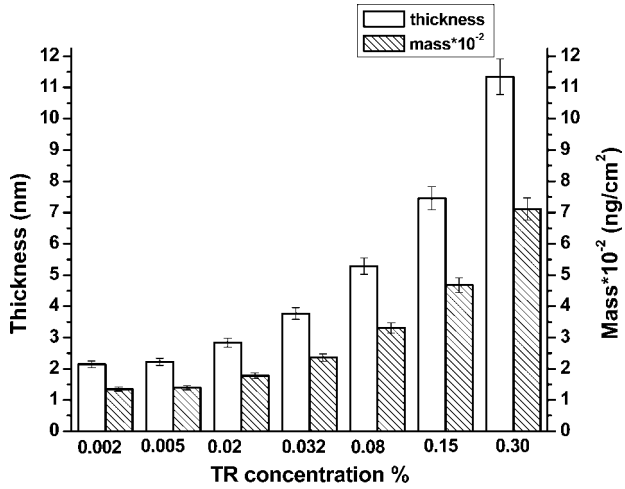

Figure 4. Changes of mass and thickness of the thearubigin adlayer on BSA surfaces at various thearubigin concentrations: (a) 0.002%; (b) 0.005%; (c) 0.02%; (d) 0.032%; (e) 0.08%; (f) 0.15%; (g) 0.30%. The thearubigin solutions were prepared in 0.01 M acetate buffer at pH = 4.9.

adsorption on the BSA surface and provides the mass and thickness of the adsorbed thearubigin adlayer on the BSA surface.

Figure 3 displays the time-resolved frequency shifts (ΔF) for the fifth overtone upon the addition of thearubigin solutions of different concentrations (ranging from 0.005% to 0.15%) onto the BSA surface at pH 4.9 and 0.01 M acetate buffer solution. With the increase of the thearubigin concentration, ΔF increases, suggesting the increase of adsorbed mass on the basis of the Sauerbrey equation. To obtain a more precise picture of thearubigin adsorption behaviors, the thearubigin adsorbed mass and the thickness of the thearubigin adlayer, based on the Voigt model, were calculated and shown in **Figure 4**. Increasing thearubigin concentration from 0.002% to 0.300% leads to increases in both thickness (i.e., from 2.1 to 11.3 nm) and mass (i.e., from 134.7 to 711.1 ng/cm^2) of the adsorbed thearubigin adlayer.

The equilibrium of adsorption is a fundamental property of the solute−surface interaction because the adsorption process will continue until a thermodynamic equilibrium of the solute concentration is reached. The equilibrium at a given temperature is usually presented with an isotherm, which is the plot of the mass of the adsorbed solute versus the solute concentration. The adsorption isotherm is useful in predicting the performance of an adsorption system. Either the Langmuir isotherm or the

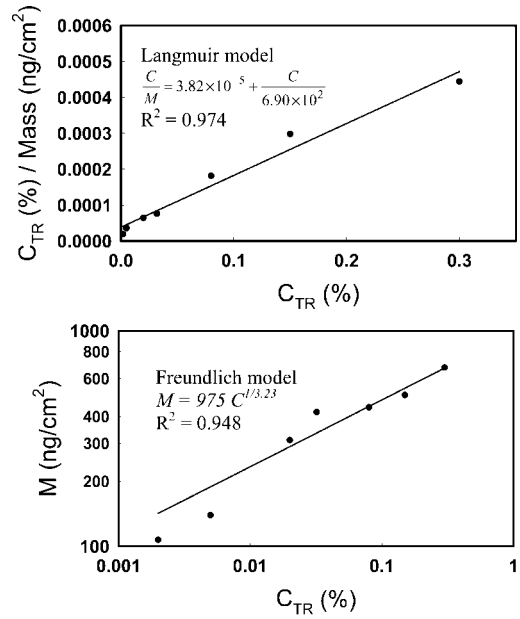

Figure 5. Adsorption isotherm of thearubigin onto the BSA surface fitted to the Langmuir model (top) and the Freundlich model (bottom).

Freundlich isotherm may be used to describe the adsorption isotherm of thearubigin onto the BSA surface, which can be determined from the changes of the adsorbed mass of thearubigin against thearubigin concentration. The Langmuir model assumes that (1) the adsorbed layer should be a monolayer, (2) there are finite numbers of identical adsorption sites on the surface, and (3) the adsorption ability of a solute to each of these sites is independent of the occupation of neighboring sites (*29*). This model is useful when there are strong specific interactions between the surface and the adsorbate. The driving force for the adsorption is the concentration of the solute, and the Langmuir isotherm can be described by the equations (*29*):

$$M = \frac{M_m KC}{1 + KC} \tag{5}$$

$$\frac{C}{M} = \frac{1}{KM_m} + \frac{1}{M_m}C \tag{6}$$

where C is the concentration of the adsorbate solution, M is the amount of adsorbate on the adsorbent, K is a direct measure of the intensity of the adsorption process, and M_m is a constant related to the area occupied by a monolayer of adsorbate, reflecting the adsorption capacity. The experimental data of thearubigin adsorption on the BSA surface give a satisfactory fit to the Langmuir model with a correlation coefficient of 0.9735, as shown in **Figure 5** (top), indicating that the Langmuir model can be used to describe the thearubigin adsorption on the BSA surface. M_m, which indicates the absorption capacity, and K, which reflects the intensity of adsorption process, can be estimated from the slope and intercept of the plot of C/M versus C/M_m and are equal to 690 ± 51 ng/cm^2 and 38.0 ± 5.6, respectively.

For comparison, we also fit the thearubigin adsorption isotherm with the Freundlich model, which can be described as

$$M = K_f C^{1/n} \tag{7}$$

The results of K_f and n estimated from the fitting to eq 7 are 975 ± 97 and 3.23 ± 0.42, respectively. The fit to experimental

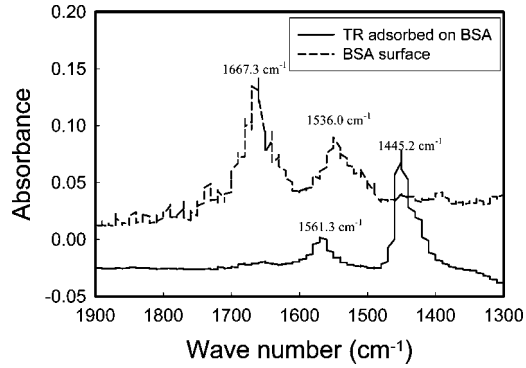

Figure 6. FTIR spectra of the pure BSA surface (dashed line) and the BSA surface with adsorbed thearubigin molecules (solid line).

data using the Freundlich model is less satisfactory compared with the Langmuir model, as shown in **Figure 5**. The Freundlich model is an empirical model and predicts infinite adsorption at infinite concentration. At low thearubigin concentration, although the distribution of thearubigin on the BSA may not be homogeneous due to the broad molecular weight dispersity of thearubigin, which ranges from 1000 to 40000 Da, the better fit of the thearubigin adsorption isotherm using the Langmuir model rather than the Freundlich model may indicate that the thearubigin adsorption onto the BSA surface is mainly governed by specific and strong interactions, and the Langmuir adsorption process may be less disturbed by the heterogeneity of binding of thearubigin on the BSA surface. Thearubigin is a polar molecule containing a large amount of hydroxyl groups as well as some carboxyl groups, which can form specific and strong interactions with BSA molecules through both hydrogen bonding and electrostatic interaction. However, at higher thearubigin concentration, large molecules may occupy more than one adsorption site than small ones. Two competing effects, the heterogeneity of the thearubigin molecules bound on BSA surface and the specific interactions between thearubigin and BSA, may cause good fits of the data by the Freundlich model at higher thearubigin concentration.

To prove the existence of hydrogen bonding between the adsorbed thearubigin molecules and BSA surfaces, FTIR spectra of BSA surfaces with and without the thearubigin adsorption were collected, as shown in **Figure 6**. The FTIR spectrum of the pure BSA surface displays two characteristic bands at 1666 and 1546 cm^{-1}. The 1666 cm^{-1} (amide I) band arises predominantly from the protein amide C═O stretching vibrations, and the 1546 cm^{-1} (amide II) band is due to the amide N−H bending vibrations and C−N stretching vibrations (*25*). The positions of amide bands I and II in the thearubigin-adsorbed BSA surface show a remarkable shift from 1667.3 to 1561.3 cm^{-1} ($\Delta\bar{\nu} = 106.0$ cm^{-1}) and from 1536.0 to 1445.2 cm^{-1} ($\Delta\bar{\nu} = 90.8$ cm^{-1}), respectively, after thearubigin adsorption. The significant peak position shifts observed in the amide I and amide II bands may be attributed to hydrogen bonding between thearubigin and BSA molecules, suggesting that the hydrogen bonding may occur between the phenolic hydroxyl groups in thearubigin and the functional groups (i.e., amide groups) of the BSA.

Our previous studies on EGCG binding to the BSA surface suggest that the main driving force between them is through hydrophobic interaction, which can be verified by temperature-dependent QCM-D measurements for 20 mM EGCG at 25, 30, and 35 °C (*25*). In that case, a higher adsorbed EGCG mass is found at the higher temperature. Here we have also carried out temperature-dependent QCM-D measurements for the adsorption of 0.032% thearubigin solution on the BSA surface. However, we find that, even at temperatures below the critical denaturing temperature of BSA (i.e., 60 °C), the increase of temperature actually decreases the amount of both thickness and mass of the thearubigin adlayer, as shown in **Figure 7a**. This result indicates that the hydrophobic interaction is not the dominant factor associated with the binding between thearubigin and BSA, simply because the hydrophobic interaction usually increases with the increase of temperature (*31*), which is opposite to the experimental results obtained regarding the changes of the adsorbed mass and thickness of thearubigin with temperature.

Effect of pH. To investigate the possible role of electrostatic interaction involved in the binding between thearubigin and BSA, in addition to the experiments performed at pH 4.9, we also conducted QCM-D measurements at pH values of 7.0 and 3.0, where BSA carries negative and positive charges, respectively. The mass and thickness of the adsorbed thearubigin adlayer on the BSA surface at pH 7.0, 4.9, and 3.0 are compared in **Figure 7b**. As discussed above, the hydrophobic interaction, even at the isoelectric point (p*I*) of BSA, is not the dominant factor for thearubigin adsorption. The significantly higher or lower adsorbed thearubigin mass and thickness at pH 3 or 7 suggest that the electrostatic interaction between BSA surface charges and charges existing in thearubigin plays a significant role in their interactions. At pH 3, the maximum adsorbed thearubigin mass and thickness indicate the existence of strong electrostatic attraction between the positively charged BSA surface and the negatively charged thearubigin molecules. On the other hand, the minimum adsorbed thearubigin mass and thickness at pH 7 may arise from the electrostatic repulsion between the negatively charged protein surface and the negatively charged thearubigin molecules. One notes from the possible dimeric structure of thearubigin molecules shown in **Figure 1** that thearubigin molecules carry a negatively charged carboxyl group (*5*).

Effect of Salt Concentration. To further understand the nature of interactions between thearubigin and BSA, we also studied the effects of salt concentration on the binding of thearubigin molecules on BSA surfaces. **Figure 7c** displays the changes of adsorbed mass and thickness of the thearubigin adlayer on BSA surfaces as a function of salt concentration. At pH 4.9, when the acetate buffer concentration increases from 0.001 to 0.100 M, both adsorbed mass and thickness increase. On the other hand, as the salt concentration increases above 0.1 M, both adsorbed mass and thickness decrease. These results indicate that salt concentration has complex effects on the electrostatic interaction between protein BSA and thearubigins. Similar salt concentration effects were also observed in the electrostatic interaction between some proteins and certain polyelectrolytes (*32*, *33*).

The protein molecules are essentially amphoteric polyelectrolytes, containing both positive and negative charges. Therefore, there simultaneously exist electrostatic attraction and electrostatic repulsion between the charges in protein molecules and thearubigin molecules. The electrostatic attraction and electrostatic repulsion may be related to the average distance between the protein's positive sites and thearubigin's negative sites (R_+), the average distance between the protein's negative sites and thearubigin's negative sites (R_-), and the Debye length (R_d) through the equation:

$$U = -\frac{Q_p}{2\epsilon}\left(\frac{Q_+}{R_+}e^{-R_+/R_d} - \frac{Q_-}{R_-}e^{-R_-/R_d}\right) \quad (8)$$

where U is the potential energy for the electrostatic interaction, Q_p is the charge of thearubigin associated with the protein molecule which contains Q_+ positive charges and Q_- negative

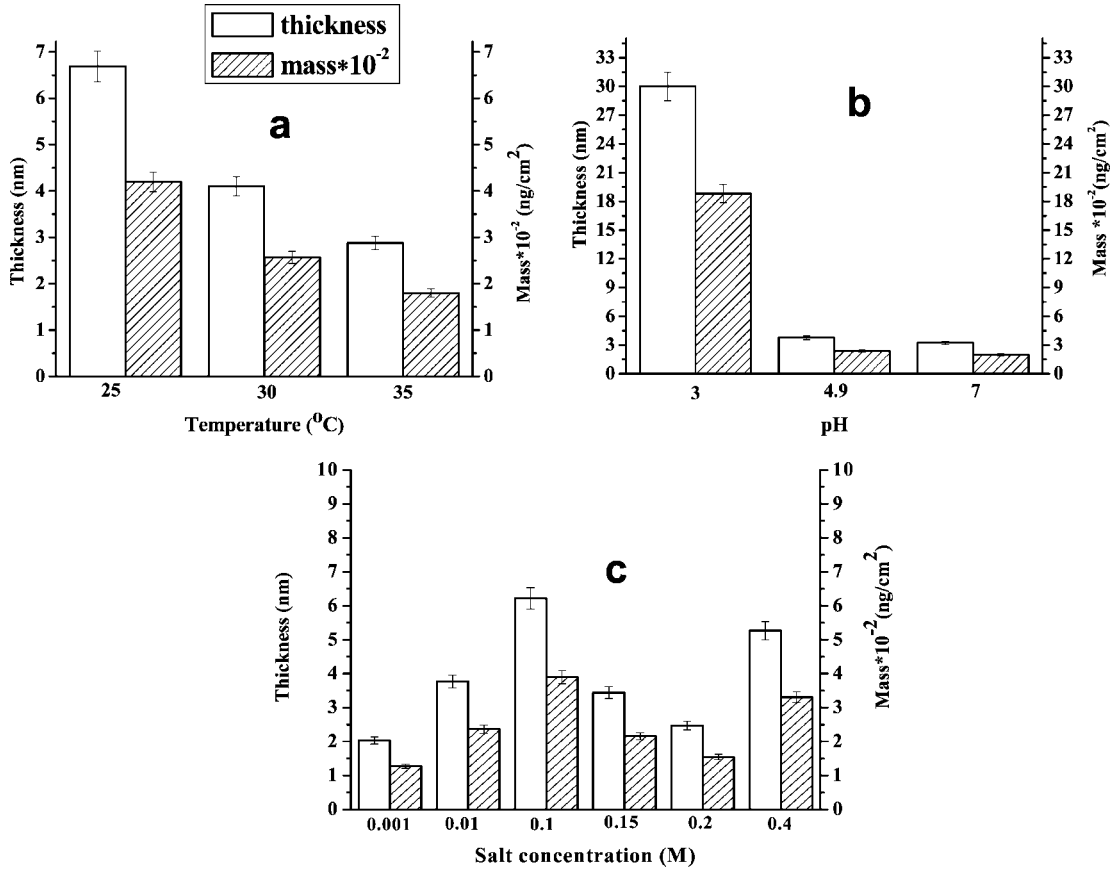

Figure 7. Changes of mass and thickness of the 0.032% thearubigin adlayer on BSA surfaces (a) at various temperatures (25, 30, and 35 °C) (0.01 M acetate buffer at pH = 4.9), (b) at various pH values (salt concentration = 0.01 M), and (c) at different acetate buffer concentrations (pH = 4.9).

charges, and ϵ is the dielectric constant. If Q_+, Q_-, R_+, and R_- are independent from salt concentration (I), the increase of salt concentration leads to Coulombic screening through influencing R_d ($R_d \approx 0.3/I^{1/2}$). During the thearubigin adsorption on the BSA surface, at lower salt concentrations, there may be $R_+ < R_d < R_-$, and the increase of salt concentration is mainly to screen the electrostatic repulsion but not disturb the electrostatic attraction between thearubigin and the BSA surface. Consequently, the total interactions will be enhanced with increasing salt concentration. This salt concentration-enhanced effect thus increases the thearubigin adsorbed mass on the BSA surface when I increases from 0.001 to 0.1 M. On the contrary, when I is above 0.1 M, there may be $R_d < R_+ < R_-$, and the added salt can screen both electrostatic attraction and repulsion significantly owing to the higher salt concentration. Therefore, the increase in I beyond 0.1 M leads to the gradually reduced amount of thearubigin molecules adsorbed on the BSA surface. However, when I is further increased to 0.4 M, the addition of thearubigin may promote the formation of a certain type of complex with BSA, resulting in an increase in the amount of thearubigin adsorbed on the BSA surface.

CONCLUSION

In summary, the adsorption of thearubigin molecules on the BSA surface was monitored in real time through the simultaneous measurements of the shifts in both resonance frequency and energy dissipation using QCM-D. The adsorbed thearubigin masses and thicknesses under different physicochemical conditions, such as thearubigin concentration, temperature, pH, and salt concentration, were calculated using the Voigt model. Our results suggest that specific interactions, such as electrostatic interaction and hydrogen bonding, are the dominant forces in thearubigin−BSA interactions. There are electrostatic attraction and repulsion between BSA protein and thearubigin. The maximum and minimum interactions between thearubigin and BSA occur at pH below and higher than the pI of the protein, suggesting the existence of strong electrostatic interaction between the negatively charged thearubigin carboxyl group and either positively charged or negatively charged BSA molecules depending on the pH. The existence of electrostatic interaction is also confirmed by the complex salt concentration effects: the adsorbed mass and thickness of the thearubigin adlayer estimated from the Voigt model confirm that the adsorption of thearubigin on the BSA surface is favored by the increase of salt concentration from 0.001 to 0.1 M. Further increase of salt concentration from 0.1 to 0.2 M hinders thearubigin adsorption and causes the formation of a thinner thearubigin adlayer. Hydrogen bonding is another dominant force in the thearubigin−BSA interactions, as evidenced by the large BSA band position shifts for both amide I and amide II before and after thearubigin adsorption in FTIR spectra. The adsorption isotherm for thearubigin adsorption on BSA can be better described by the Langmuir model than the Freundlich model. This research will help us to better understand the mechanism that controls the polyphenol binding to proteins and can be extended to studies of bindings between drugs and receptor proteins.

LITERATURE CITED

(1) Graham, H. N. Green tea consumption and polyphenol chemistry. *Prev. Med.* **1992**, *21*, 334–350.

(2) (a) Arts, M. J. T. J.; Haenen, G. R. M. M.; Wilms, L. C.; Beetstra, S. A. J. N.; Heijnen, C. G. M.; Voss, H. P.; Bast, A. Interaction between flavonoids and proteins: Effect on the total antioxidant capacity. *J. Agric. Food Chem.* **2002**, *50*, 1184–1187. (b) Ferruzzi, M. G.; Green, R. J. Analysis of catechins from milk-tea beverages by enzyme assisted extraction followed by high performance liquid chromatography. *Food Chem.* **2006**, *91*, 484–491.

(3) Liang, Y. C.; Chen, Y. C.; Lin, Y. L.; Lin-Shiau, S. Y.; Ho, C.-T.; Lin, J. K. Suppression of extracellular signals and cell proliferation by the black tea polyphenol, theaflavin-3,3′-digallate. *Carcinogenesis* **1999**, *20*, 733–736.

(4) Liang, Y. C.; Lin, J. K. Cancer chemoprevention by tea polyphenols. *Proc. Natl. Sci. Counc., Repub. China, Part B: Life Sci.* **2000**, *24*, 1–13.

(5) Haslam, E. Thoughts on thearubigins. *Phytochemistry* **2003**, *64*, 61–73.

(6) Yao, L. H.; Jiang, Y. M.; Caffin, N.; Arcy, B. D.; Datta, N.; Liu, X.; Singanusong, R.; Xu, Y. Phenolic compounds in tea from Australian supermarkets. *Food Chem.* **2006**, *96*, 614–620.

(7) Shiraki, M.; Hara, Y.; Osawa, T.; Kumon, H.; Nakayama, T.; Kawakishi, S. Antioxidative and antimutagenic effects of theaflavins from black tea. *Mutat. Res.* **1994**, *323*, 29–34.

(8) Leung, L. K.; Su, Y.; Chen, R.; Zhang, Z.; Huang, Y.; Chen, Z. Y. Theaflavins in black tea and catechins in green tea are equally effective antioxidants. *J. Nutr.* **2001**, *131*, 2248–2251.

(9) Miller, N. J.; Castelluccio, C.; Tijburg, L.; Rice-Evans, C. The antioxidant properties of theaflavins and their gallate esters-radical scavengers or metal chelators. *FEBS Lett.* **1996**, *392*, 40–44.

(10) Lin, Y. L.; Tsai, S. H.; Lin-Shiau, S. Y.; Ho, C.-T.; Lin, J. K. Theaflavin-3,3′-digallate from black tea blocks the nitric oxide synthase by down-regulating the activation NF-kB in macrophages. *Eur. J. Pharmacol.* **1999**, *367*, 379–388.

(11) Yoshino, K.; Hara, Y.; Sano, M.; Tomita, I. Antioxidative effects of black tea theaflavins and thearubigin on lipid peroxidation of rat liver homogenates induced by tert-butyl hydroperoxide. *Biol. Pharm. Bull.* **1994**, *17*, 146–149.

(12) Gupta, S.; Chaudhuri, T.; Seth, P.; Ganguly, D. K.; Giri, A. K. Antimutagenic effects of black tea (World Blend) and its two active polyphenols theaflavins and thearubigins in *Salmonella* assays. *Phytother. Res.* **2002**, *16*, 655–661.

(13) Charlton, A. J.; Baxter, N. J.; Khan, M. L.; Moir, A. J. G.; Haslam, E.; Davies, A. P.; Williamsom, M. P. Polyphenol-peptide binding and precipitation. *J. Agric. Food Chem.* **2002**, *50*, 1593–1601.

(14) Jöbstl, E.; O'Connell, J.; Fairclough, J. P. A.; Williamsom, M. P. Molecular model for astrigency produced by polyphenol/protein interactions. *Biomacromolecules* **2004**, *5*, 942–949.

(15) Charlton, A. J.; Haslam, E.; Williamson, M. Multiple conformations of the prolne/epigallocatechin gallate complex determined by time-averaged nuclear Overhauser effects. *J. Am. Chem. Soc.* **2002**, *124*, 9899–9905.

(16) Hertog, M. G. L.; Swertman, P. M.; Fehily, A. M.; El-wood, P. C.; Kromhout, D. Antioxidant flavonols and ischemic heart disease in a Welch population of men: The Caerphilly study. *Am. J. Clin. Nutr.* **1997**, *85*, 1489–1494.

(17) Brown, J. R.; Shockley, P. *Lipid-Protein Interactions*, 6th ed.; Jost, P. C., Griffith, O. H., Eds.; John Wiley & Sons: New York, 1982.

(18) Peters, T. J. *All about Albumin Biochemistry, Genetics, and Medical Application*; Academic Press: San Diego, 1996.

(19) Sauerbrey, G. Verwendung von schwingquarzen zur wägung dünner schichten und zur mikrowägung (The use of quartz oscillators for weighing thin layers and for microweighing). *Z. Phys. A: Hadrons Nucl.* **1959**, *155*, 206–222.

(20) Carrigan, S. D.; Scott, G.; Tabrizian, M. Real-time QCM-D immunoassay through oriented antibody immobilization using cross-linked hydrogel biointerface. *Langmuir* **2005**, *21*, 5966–5973.

(21) Janshoff, A.; Steinem, C.; Sieber, M.; el Bayâ, A.; Schmidt, M. A.; Galla, H.-J. *Eur. Biophys. J.* **1997**, *26*, 261–270.

(22) Muramatsu, H.; Dicks, J. M.; Tamiya, E.; Karube, I. Piezoelectric crystal biosensor modified with protein A for determination of immunoglobulins. *Anal. Chem.* **1987**, *59*, 2760–2763.

(23) Höök, F.; Rodahl, M.; Fredriksson, C.; Brzezinski, P.; Keller, C. A.; Voinova, M.; Krozer, A.; and Kasemo, B. Simultaneous frequency and dissipation factor QCM measurements of biomolecular adsorption and cell adhesion. *Faraday Discuss.* **1997**, *107*, 229–246.

(24) Liu, M.; Zhang, Y.; Yang, Q.; Xie, Q.; Yao, S. Monitoring and estimation of kinetics parameters in the binding process of tannic acid to bovine serum albumin with electrochemical quartz crystal impedance system. *J. Agric. Food Chem.* **2006**, *54*, 4087–4094.

(25) Wang, X. Y.; Ho, C.-T.; Huang, Q. R. Investigation of adsorption behavior of (−)-epigallocatechin gallate on bovine serum albumin surface using quartz crystal microbalance with dissipation monitoring. *J. Agric. Food Chem.* **2007**, *55*, 4987–4992.

(26) Patel, N.; Davies, M. C.; Heaton, R. J.; Roberts, C. J.; Tendler, S. J. B.; Williams, P. A scanning probe microscopy study of the physisorption and chemisorption of protein molecules onto carboxylate terminated self-assembled monolayers. *Appl. Phys. A: Mater. Sci. Process.* **1998**, *66*, S569–S574.

(27) Voinova, M. V.; Rodahl, M.; Jonson, M.; Kasemo, B. Viscoelastic acoustic response of layered polymer films at fluid-solid interfaces: continuum mechanics approach. *Phys. Scr.* **1999**, *59*, 391–396.

(28) Höök, F.; Kasemo, B.; Nylander, T.; Fant, C.; Sott, K.; Elwing, H. Variations in coupled water, viscoelastic properties, and film thickness of a Mefp-1 protein film during adsorption and cross-linking: A quartz crystal microbalance with dissipation monitoring, ellipsometry, and surface plasmon resonance study. *Anal. Chem.* **2001**, *73*, 5796–5804.

(29) Langmuir, I. The adsorption of gases on plane surfaces of glass, mica and platinum. *J. Am. Chem. Soc.* **1918**, *40*, 1361–1402.

(30) Rao, R. M.; Marshall, W. E.; Losso, J. N.; Chilton, N. G. Freundlich adsorption isotherms of agricultural by-product-based powered activated carbons in a geosmin-water system. *Bioresour. Technol.* **2002**, *85*, 131–135.

(31) Relkin, P. Thermal unfolding of β-lactoglobulin, α-lactalbumin, and bovine serum albumin. A thermodynamic approach. *Crit. Rev. Food Sci. Nutr.* **1996**, *36*, 565–601.

(32) Seyrek, E.; Dubin, P. L.; Tribet, C.; Gamble, E. A. Ionic strength dependence of protein-polyelectrolyte interactions. *Biomacromolecules* **2003**, *4*, 273–282.

(33) Hattori, T.; Hallberg, R.; Dubin, P. L. Roles of electrostatic interaction and polymer structure in the binding of β-lactoglobulin to anionic polyelectrolytes: Measurement of binding constants by Frontal analysis continuous capillary electrophoresis. *Langmuir* **2002**, *16*, 9738–9743.

Received for review July 25, 2007. Revised manuscript received October 7, 2007. Accepted October 12, 2007. This project was supported by the Center for Advanced Food Technology (CAFT) and in part by the USDA-NRI.

JF072236T